of the F and H centers could be close to each other. As a result one might look for effects of one center on the other. Two experiments have been attempted both of which failed to find such an interaction. In one case irradiation in the H-absorption band failed to produce F-center luminescent emission which should have occurred if the H center transferred energy to the F center.[17] In the other experiment no effect was found on the polarization of the F center if the H centers were turned so that most of them were oriented in one direction rather than being randomly distributed.[10] The details of the spin-resonance spectrum also argue against a close proximity of the F and H centers.[18] It thus seems likely that the centers move apart even at these low temperatures. One mechanism may be the propagation of the H center along the row of halide ions in the $\langle 110 \rangle$ directions. The details of such a motion have, however, not been investigated.

ACKNOWLEDGMENT

It is a pleasure to acknowledge that the stimulation for this work arose from discussions with Professor David L. Dexter and from examination of his paper prior to publication.

[17] W. D. Compton and C. C. Klick (unpublished work).

[18] W. Känzig (private communication).

PHYSICAL REVIEW VOLUME 120, NUMBER 3 NOVEMBER 1, 1960

Nuclear Quadrupole Resonance in Superconducting Gallium*

R. H. HAMMOND AND W. D. KNIGHT
Department of Physics, University of California, Berkeley, California

(Received June 13, 1960)

The nuclear quadrupole resonance (NQR) of Ga^{69} is investigated between 0.8 and 4.2°K. (The superconducting critical temperature is 1.084°K.) Progressive saturation of the resonance is produced at increasing rf power levels of a frequency-modulated marginal oscillator. The nuclear spin-lattice relaxation rate $1/T_1$ (sec^{-1}) is approximately $\frac{1}{2}T$ (°K) in the normal state. The contact part of the hyperfine interaction appears to be predominant in producing relaxation. Although the saturation method does not permit a precise determination of the constant of proportionality, the comparison of normal and superconducting relaxation rates is considerably more reliable. The rf fields are assumed to obey the London law of penetration, and an average rf field is determined in the superconductor. The relaxation rate shows a maximum enhancement by a factor 1.8 at approximately 0.95 T_c, a result which agrees with that obtained by Slichter and Hebel, and Redfield for the nuclear magnetic resonance of aluminum, and which serves as an additional experimental justification for certain features of the Bardeen-Cooper-Schrieffer theory of superconductivity. Unsaturated signal intensities in normal and superconducting states furnish a basis for estimating the penetration depth in superconducting metal spheres: $\lambda(0) = 1200$ A for an average particle diameter of 2.7 μ. The NQR frequency of Ga in the superconductor shifts by $(+)5\times10^{-5}$ of the normal frequency [the corresponding result for indium is found to be approximately $(-)10^{-2}$]. This means that the contribution of the conduction electrons to the average nuclear quadrupole coupling is modified by the rearrangement of the conduction band in the superconductor. It is demonstrated that, if the quadrupole term in the hyperfine interaction were to predominate, the spin relaxation rate in the superconductor would have a temperature dependence like that of the ultrasonic attenuation.

I. INTRODUCTION

IN searching for nuclear quadrupole resonance (NQR) in metals one anticipated the possibility of observing the resonance in a superconducting metal. Since NQR is performed in zero magnetic field (except for a small rf field), the requirements on the particle size are much easier to satisfy than they are for an experiment on the nuclear magnetic resonance (NMR) in superconductors.[1–3] Following the discovery of the NQR in gallium,[4] the present work became possible. In succeeding sections we shall discuss the nuclear spin relaxation rate and the penetration depth in superconducting gallium. A separate report will be made on these effects in indium,[5] including a more complete discussion of the observed NQR frequency shift in both superconductors.

The relaxation mechanism in metals is based on interactions between nuclear spins and conduction electrons near the Fermi surface. Since, in any theory of superconductivity, rearrangements take place in the conduction band, it is to be expected that the relaxation rate will change when the metal becomes superconducting. It was in fact found experimentally that the rate increases to a maximum at approximately ninety-

* Supported in part by the U. S. Office of Naval Research and the Alfred P. Sloan Foundation.

[1] F. Reif, Phys. Rev. **102**, 1417 (1956); **106**, 208 (1957).

[2] W. D. Knight, G. Androes, and R. Hammond, Phys. Rev. **104**, 852 (1956).

[3] G. M. Androes and W. D. Knight, Phys. Rev. Letters **2**, 386 (1959).

[4] W. D. Knight, R. R. Hewitt, and M. Pomerantz, Phys. Rev. **104**, 271 (1956).

[5] R. R. Hewitt and W. D. Knight, Phys. Rev. Letters **3**, 18 (1959).

five percent of the transition temperature; at lower temperatures a further decrease was noted.

The result is in agreement with NMR experiments on aluminum.[6-8] The latter involved a field cycling method, which allowed the measurements to be made in the normal state, following periods of relaxation in the superconducting state. By measuring the relaxation rate under steady-state conditions, we avoid the problems of trapped flux and supercooling which are associated with the field cycling of a superconductor.

The results of the experiments on aluminum and on gallium (reported here) are both in agreement with a calculation of the relaxation rate based on the Bardeen, Cooper, Schrieffer (BCS)[9] theory of superconductivity. The (contact) magnetic hyperfine interaction between the nucleus and the conduction electrons is assumed to predominate over other relaxation processes. However, we note that a nuclear quadrupole interaction with conduction electrons may under certain circumstances contribute to the relaxation rate[10]: As a further consequence of the BCS theory, it will be shown in a later section that the quadrupole contribution to the rate drops exponentially to zero with an infinite slope at $T=T_c$, the superconducting transition temperature. This difference in the magnetic and quadrupole interactions depends upon their respective behaviors under the operation of time reversal.

It is somewhat difficult to observe the NQR in a superconductor because the experimental rf field is attenuated in the sample (Meissner effect). However, the maximum attenuation on this account is less than a factor of ten (which is easily tolerated), and furthermore the effect may be used to advantage by calculating from it the superconducting penetration depth.

The NQR frequency is observed to change below the transition temperature. This is consistent with the assumption that part of the quadrupole energy arises from a static interaction between the nuclear quadrupole moment and the conduction electrons.

NQR in Gallium

We are concerned with the process of detection of radio frequency resonance absorption in crystals which possess energy levels determined by the nuclear quadrupole moment and the crystalline electric field gradients at the nucleus. These are caused by crystalline anisotropy of the surrounding charge distributions. In general, one must consider ionic charges at lattice points, covalent bonds, and (in a metal) the conduction electrons.

The subject of NQR has been reviewed extensively.[11] In his thesis, Pomerantz[12] discusses gallium in particular. We summarize here some pertinent facts.

Gallium exists in two isotopes, each of which has a nuclear spin $I=\frac{3}{2}$. The quadrupole coupling produces two energy levels, which are separated by a frequency

$$\nu=e^2qQ(1+\eta^2_3)^{\frac{1}{2}}/2h,$$

where $q=q_{zz}$, the maximum component of the electric field gradient tensor, eQ is the nuclear electric quadrupole moment, and the asymmetry parameter $\eta=(q_{xx}-q_{yy})/q_{zz}$. The relative abundances of the two isotopes, Ga^{69} and Ga^{71}, are 60% and 40%, respectively; at 4.2°K, the NQR frequencies are 11.31 Mc/sec and 7.13 Mc/sec. The present work is concerned primarily with observations on the Ga^{69} isotope.

In succeeding sections we shall discuss the experimental apparatus, the measurements, the theory of relaxation, and experimental results.

II. EXPERIMENTAL APPARATUS

Resonance Equipment

The marginal oscillator was used in previous experiments on gallium[4,12]; some additional features were necessary for the performance of the present experiments.

Calibration

Since this experiment involved the measurement of signal amplitudes, a means of calibration was needed. Two different calibrators, functioning as primary and secondary standards, were used. The latter employed a triode, as described by Watkins[13,14]: A voltage at the modulation frequency is applied to the grid, thereby changing the plate resistance; the plate resistance is loosely coupled to the tank circuit of the marginal oscillator; the variation in plate resistance is equivalent to a modulated nuclear resonance absorption.

The other calibrator employs a mechanical chopper,[12] which switches a fixed resistance across the tank circuit once each cycle of modulation frequency. The chopper type of calibrator has the advantage of stability: It consists only of resistors, capacitors, and an off-on device. The tube calibrator, on the other hand, is subject to changes in tube characteristics. However, the chopper calibrator has the practical disadvantage of a limited dynamic range (several fixed amplitudes could be obtained by switching among different resistors, but this is inconvenient at radio frequencies). In practice, the two calibrators were used in conjunction

[6] L. C. Hebel and C. P. Slichter, Phys. Rev. **113**, 1504 (1959).
[7] A. Redfield, Phys. Rev. Letters **3**, 85 (1959).
[8] Y. Masuda and A. Redfield, Bull. Am. Phys. Soc. **5**, 176 (1960).
[9] J. Bardeen, L. N. Cooper, and J. R. Schrieffer, Phys. Rev. **108**, 1175 (1957).
[10] A. H. Mitchell, J. Chem. Phys. **26**, 1714 (1957).
[11] T. P. Das and E. L. Hahn, in *Solid-State Physics*, edited by F. Seitz and D. Turnbull (Academic Press, Inc., New York, 1958), Suppl. No. 1.
[12] M. Pomerantz, thesis, University of California, 1958 (unpublished).
[13] G. Watkins, thesis, Harvard University, 1953 (unpublished).
[14] R. V. Pound, *Progress in Nuclear Physics* (Butterworths Scientific Publications, Ltd., London, 1952), Vol. 2, p. 21.

—the tube type for calibrating the intensity of the resonance signals and the other type for checking on the first. Since the experiment extended over a period of many weeks, this sort of reliable standard was an indispensable part of the equipment. The tube calibrator was used in order to establish the fact that the linearity of the whole system was better than 3% under all conditions of operation.

Phase

Since the phase of the detected resonance signal varies with oscillator level, the correct phase setting of the coherent detector must be determined at each rf level. This was accomplished by making a series of runs for every level setting. At least three preliminary runs were made, in addition to the final one at the selected best phase. The signal strengths were usually reproducible to within a 2% variation for identical conditions over the entire period of experimentation.

Frequency Measurement

In order to avoid exposing the superconductor to the square-wave modulating field which is usually employed in NQR experiments, the modulation of the absorption was accomplished alternatively by modulating the frequency of the marginal oscillator. The modulation frequency was 100 cps, and the rf frequency excursion approximately 3 kc/sec, peak-to-peak. The frequency was measured by means of an events-per-second frequency counter, the counting interval being exactly one second. Each measurement represented, therefore, an average rf frequency over one hundred modulation periods.

Other factors, important in obtaining the necessary accuracy, included monitoring the rf level and the amplitude of the frequency excursion. Since two percent accuracy is rather high for measurements of this sort, we show pictures of two runs (Fig. 1) in the normal and superconducting states, demonstrating the very high signal-to-noise ratio which permits us to achieve the accuracy which is claimed.

Cryogenic Equipment

Cryostat

Temperatures below 1°K were obtained by pumping on liquid helium through a small (0.020-in. diam) orifice. The arrangement included double Dewars for liquid nitrogen and liquid helium, respectively. The latter, which will be referred to as "the bath," was, except in one instance, kept at atmospheric pressure. Immersed in the bath was an all-metal cryostat,[15,16] which, at its lower end, consisted of two concentric brass cans, isolated by a space containing a controlled amount of exchange gas. The inner can contained liquid helium, and was suspended by a one-inch length of ($\frac{1}{8}$-in. diam) stainless steel tubing. This tube was terminated at the inner can by the 0.020-in. diam $\frac{1}{8}$-in. long constriction, which served to limit the superfluid film creep. Successively higher sections of the pumping line were larger and larger, the room-temperature end having a diameter of 2 in. This was connected through a valve and diffusion pump of comparable size to a forepump. The lowest temperature attained was 0.793°K, for which it was necessary to reduce the bath temperature to 1.6°K; with a bath temperature of 4.2°K, the lowest temperature in the inner can was 0.839°K.

The inside of the inner can was the working space, containing the rf coil wound on a Lucite form, and the sample in a glass tube which allowed liquid helium to enter, thus insuring thermal contact with the inner can.

The rf connection between the two cans (which was critical in the sense that it in part determined the heat leak to the inner can and, hence, the lowest attainable temperature) consisted of a vanadium tube (length

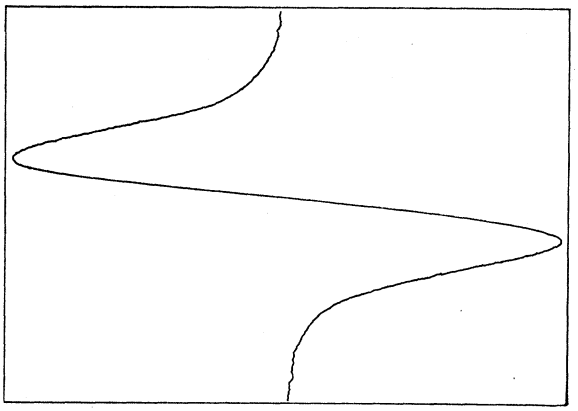

(a)

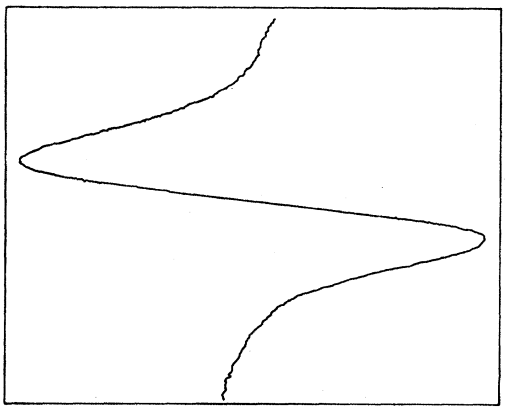

(b)

FIG. 1. (a) Run at $T=1.18$°K. Time constant$\approx$5 sec; (b) $T=0.793$°K. Time constant$\approx$5 sec. As a result of the Meissner effect, the intensity is about $\frac{1}{5}$ of the intensity in Fig. 1(a).

[15] We wish to thank Dr. N. Kurti for assistance in the design of the cryostat.

[16] Similar to the cryostat described by J. F. Cochran, D. E. Mapother, and R. E. Mould, Phys. Rev. **103**, 1657 (1956).

2.2 cm, circumference 0.8 cm, and wall thickness 0.001 in.). Vanadium was chosen because, while it is a superconductor below 4.2°K, it is also a poor heat conductor (the difference in heat conductivity between the normal and superconducting states of metals is not enough to be helpful here). The rf current passed through the two cans via platinum-soft-glass seals. The cans were sealed on with Wood's metal.

Temperature Measurement

The temperature of the helium in the inner can between 4.2 and 1.2°K was determined from the vapor pressure; calibrated resistors were used at lower temperatures.

The vapor pressure was measured via the tube containing the rf lead. This tube was connected with the pumping line just above the outer can. In this way one avoided measuring the pressure in a line supporting a gradient in pressure. Below the lambda point, the pressure gradient in the constriction was negligible. The actual pressure measurement involved a mercury or oil manometer, or a McLeod gauge.

In order to obtain accurate temperatures below 1.2°K, one commonly measures the paramagnetic susceptibility of a suitable salt. However, it was sufficient for this work (accuracy about 0.001°K) to use a certain type of carbon resistor, which had previously been calibrated against a paramagnetic salt in independent experiments.[17–19] In order to verify the accuracy of this method, we compared our value of T_c (1.084°K) with the result of Seidel and Keesom[20] (range 1.084 to 1.090, average 1.078°K). It is not known whether the small differences between our result and theirs arises from differences in the properties of the samples or alternatively from differences in the temperature calibrations.

Two Speer resistors were fastened outside of the inner can with G.E. 7031 cement. The resistances were measured with a potentiometer (measuring current 1 microamp).

Temperature Regulation

It sometimes required between 3 and 5 hours to accumulate data at a given temperature. Therefore, in order to smooth out drifts in temperature from variations in pumping speed and from variations in rf power levels, a temperature regulator was needed. At temperatures above 1.5°K, a commercial manostat operated satisfactorily. However, at the lower temperatures a different scheme was employed. This included an ac Wheatstone bridge (one of the Speer resistors in the measuring arm), a null detector (consisting of a narrow-band amplifier and phase-sensitive detector), and a dc power amplifier supplying power to a noninductive heater on the inner can. Similar circuits have been described elsewhere.[21]

Sample

The supplier of the sample (Aluminum Company of America) stated the purity to be 99.999%. In its final form, the sample consisted of a dry powder mixture of one quarter gallium and three quarters quartz powder of comparable particle size. Previously made samples, in which the gallium was suspended in oil or paraffin wax, were found to include strains which produced a broadening of the NQR signal at low temperatures, and a severe loss in intensity.

The gallium particles were made by exposing the molten metal to ultrasonic radiation in a volatile organic liquid containing a stabilizing agent. The mechanism of emulsification of liquid metals has been described by many authors.[22]

Microphotographs of the sample were made in order to analyze the size distribution. Each particle was observed to be very nearly spherical. The diameters ranged between 1.5 and 3.8 microns; approximately ninety percent of the diameters were between 2.0 and 3.2 microns.

III. MEASUREMENTS

Saturation Method

A preferred method of determining the relaxation time T_1 would involve a pulse technique[23] which gives a direct measurement of the appropriate time. However, preliminary results of this sort were unsatisfactory at low temperatures, presumably because of transient heating effects on the sample at high rf power levels. Therefore, although some rough data were obtained by this method, the principal conclusions of the present work are based on experiments employing the well-known method of progressive saturation of the cw resonance.[24,25]

A convenient variable is the "saturation factor" Z, which is defined as the ratio n/n_0, where n is the net excess number of nuclear spins in the lower of two energy states, and n_0 is this number at equilibrium. The result of a first-order perturbation calculation is

$$n/n_0=[1+a\gamma^2H_1^2T_1g(\nu)]^{-1},$$

where γ is the nuclear magnetomechanical ratio,

[17] J. Gordon, thesis, University of California, 1958 (unpublished).
[18] V. Arp, thesis, University of California, 1959 (unpublished).
[19] D. Peterson and D. Edmonds (private communication).
[20] G. Seidel and P. H. Keesom, Phys. Rev. **112**, 1083 (1958).
[21] C. Blake, C. E. Chase, and E. Maxwell, Rev. Sci. Instr. **29**, 715 (1958).
[22] C. Bondy and K. Sollner, Trans. Faraday Soc. **32**, 556 (1936); and **31**, 843 (1935). L. Bergmann, *Ultrasonics and Their Scientific and Technical Applications* (John Wiley & Sons, Inc., New York, 1948).
[23] E. L. Hahn, Phys. Rev. **80**, 580 (1950).
[24] N. Bloembergen, E. Purcell, and R. V. Pound, Phys. Rev. **73**, 679 (1948).
[25] E. R. Andrew, *Nuclear Magnetic Resonance* (Cambridge University Press, New York, 1955).

$H_x=2H_1\cos\omega t$ is the applied rf magnetic field, T_1 is the nuclear spin-lattice relaxation time, $g(\nu)$ is the normalized shape function for the absorption, and $a=\frac{1}{2}$ for NMR; or 2 for NQR, $I=\frac{3}{2}$ in a polycrystalline specimen or axial or nonaxial symmetry.[26]

Since the observed signal is proportional to the saturation factor, the method of determining T_1 involves measurements of the resonance at progressively larger values of H_1, ranging from $Z=1$ to, say, $Z=\frac{1}{2}$ [where $a\gamma^2H_1^2T_1g(\nu)=1$].

The preceding saturation factor is not good for determining T_1 precisely.[27] However, the deviations of a correct expression from the above simple form in the absorption mode (as contrasted with the changes in behavior of the dispersion mode) are not great. If one desires merely relative values of T_1, the analysis based on the simple formula is adequate. (It was observed in the present experiments that the absorption line "saturation narrowed"[28,29]; there was also a slight maximum of the absorption intensity[29] before saturation set in.)

Response of the Marginal Oscillator

Normal State

In order to make use of the saturation factor, we must consider how it is obtained from the observed resonance. It can be shown[13] that the response of the marginal oscillator is proportional to $n\xi g(\nu)$, where ξ is the filling factor $\int H_1^2d\tau_1/\int H_1^2d\tau$. In this expression, the numerator is proportional to the energy stored in the sample metal; the denominator represents the total magnetic energy associated with the rf coil. The constant of proportionality may be determined experimentally by means of the calibrator. Thus we may say that the signal $S=n\xi g(\nu)$. The incremental signal dS appropriate to a volume element $d\tau_1$ of the sample is $dS=ng(\nu)d\xi$, where $d\xi=H_1^2d\tau_1/\int H_1^2d\tau$. Thus

$$dS=n_0g(\nu)H_1^2\left[\int H_1^2d\tau\right]^{-1}[1+2\gamma^2H_1^2T_1g(\nu)]^{-1}d\tau_1.$$

In a normal material, all of the quantities appearing in the above expression are constant throughout the sample, and the integration over the volume of the sample is trivial.

Superconducting State

However, in the superconductor, the integration is complicated by the variation of H_1 inside the metal spheres; in addition, the shape function will in general also be different near the surface of a sphere relative to its value in the interior. In a first approximation the shape function will be assumed to be constant; later on, the possible effects of its variation will be considered. We also neglect the effect on $\int H_1^2d\tau$ of the reduction in effective sample volume by the Meissner effect in the superconductor. This is reasonable, since the ratio of sample volume to coil volume is small. The error from this approximation is less than one percent. (The frequency of the tank circuit changed by only 7/10% because of the diamagnetic susceptibility of the superconductor.)

In order to evaluate the expression for the response when the sample is superconducting, we must know H_1 as a function of position in each sphere of the sample. A good approximation is provided by the solutions to London's equations.[30] At the NQR frequency for Ga, we are justified in using the quasistationary equations, since the dominant term is independent of frequency. We may furthermore use the London equation for penetration instead of the more exact relation of Pippard,[31] since the differences between the laws of penetration appear to be no more than a few percent. Pippard's equation has not been solved for a sphere.

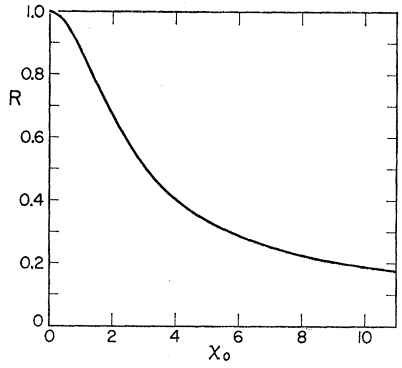

FIG. 2. Theoretical ratio of the signal in the superconductor to that in the normal metal. $\chi_0\equiv r_0/\lambda$, where r_0 is the radius of a sphere of sample, and λ is the superconducting penetration depth. Calculated on the basis of London's equations.

Signal in the Limit of No Saturation

At vanishingly small rf levels, $2\gamma^2H_1^2T_1g(\nu)\ll1$. In Appendix A, the solution for the signal strength is demonstrated. The calculations are simplified if we consider the ratio of signal in the superconductor to that in the normal metal, at the same temperature (signal in the normal metal multiplied by T_c/T for temperatures below T_c). Figure 2 shows a plot of this ratio, R, against $\chi_0=r_0/\lambda$, where r_0 is the radius of a sphere of sample, and λ is the superconducting penetration depth. Since λ is a function of the reduced temperature ($t=T/T_c$), R will be also. As a first approximation, we use the dependence of λ on t as given by the two-fluid model of superconductivity: $\chi_0=r_0(1-t^4)^{\frac{1}{2}}/$

[26] C. Dean, Phys. Rev. **96**, 1053 (1954).
[27] A. G. Redfield, Phys. Rev. **98**, 1787 (1955).
[28] D. F. Holcomb, Phys. Rev. **112**, 1599 (1958).
[29] K. Tomita, Progr. Theoret. Phys. (Kyoto) **19**, 541 (1958).
[30] F. London, *Superfluids* (John Wiley & Sons, Inc., New York, 1950), Vol. I.
[31] A. B. Pippard, Proc. Roy. Soc. (London) **A216**, 547 (1953).

$\lambda(0)$, where $\lambda(0)$ is the penetration depth at $t=0$. Figure 3 shows R vs T, fitted to the experimental points by choosing a value of $\lambda(0)=1200\pm100$ A for $r_0=1.3$ microns, the weighted average over the size distribution.

Signal during Partial Saturation

This case is considered in Appendix B. We evaluate the saturation factor in the superconductor, using the solutions of London's equations. Figure 4 shows the saturation curves for both normal and superconducting metal. It will be recalled that Z is the ratio of the partially saturated signal to the unsaturated signal.

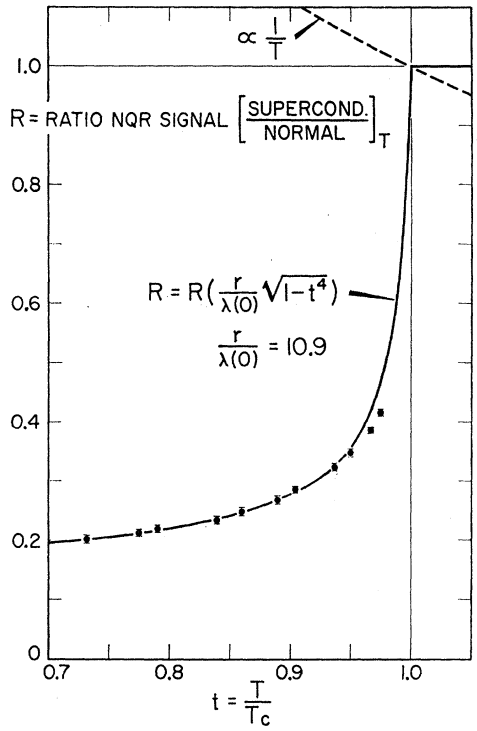

FIG. 3. The ratio of the NQR signal intensity, superconducting to normal state, vs the reduced temperature. In plotting the solid line we employ Fig. 2 and obtain a best fit to the experimental points shown by choosing $\lambda(0)=1200\pm100$ A and assuming $\lambda=\lambda(0)(1-t^4)^{-\frac{1}{2}}$. The dotted curve shows the temperature dependence of the signal intensity in the normal state.

Determination of T_1 in the Superconductor

Reduction to normal State Saturation Curve

As is shown in Fig. 4, the Meissner effect displaces the saturation curve towards larger values of H_1; the displacement of the curve depends on the value of χ_0. The two curves in the figure are drawn for the same value of T_1. Then, if we know the value of χ_0, we may map any saturation curve for the superconductor back onto the normal-state curve. T_1 can then be determined as for a normal material. We have taken the ratio H_1^N/H_1^S of the abscissas at the same ordinate in Fig. 4 in order to arrive at the set of curves (Z is the parameter) of Fig. 5. The latter plot affords a convenient means of mapping the data for the superconductor into the corresponding normal-state data; the value of χ_0 is determined from an analysis of the unsaturated signal intensities.

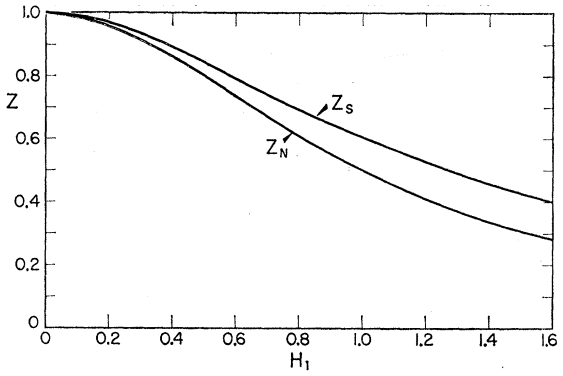

FIG. 4. The saturation factor for the normal state and the superconducting states, Z_N and Z_S. Z_N is $1/(1+cH_1^2)$, where $c=2\gamma^2T_{1g}(\nu)$. Drawn for $c=1$. Z_S is drawn for $c=1$ and $\chi_0=10$. See Appendix B.

It is to be noted that, in the range where χ_0 exceeds about 3, the correction factor H^N/H^S does not depend strongly on χ_0. It is furthermore fortunate that the particle size was such as to make χ_0 lie between 3 and 12 for all temperatures encountered in the experiments. As Fig. 5 shows, the correction factor in this range will not differ greatly among the particle sizes of the actual distribution.

Integration of the Absorption Derivative

We analyzed the data according to a scheme in which "the signal" was the height of the absorption curve at its center. It was therefore necessary to integrate the experimentally obtained derivative of the absorption. In order to perform the integration, it was necessary to determine equal frequency intervals among the random frequency markers on the recorder chart. This process, plus the actual integration by second-order interpolation, was done on a computer. The data fed

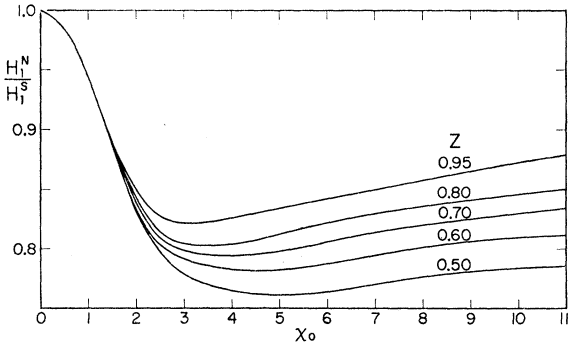

FIG. 5. The ratio, normal state to superconducting state, of the rf intensity that produces the same saturation, Z, plotted as a function of χ_0.

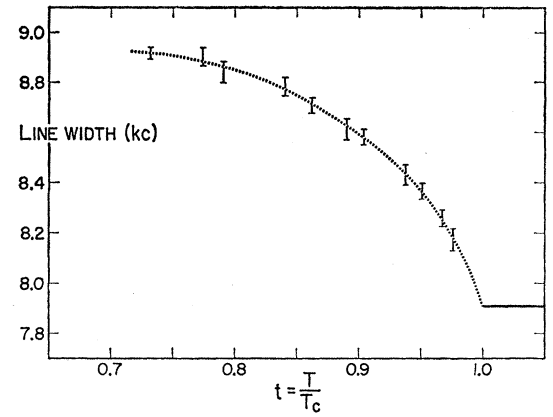

FIG. 6. The temperature dependence of the linewidth (measured between points of half-maximum absorption), through the superconducting transition.

into the computer for each chart consisted of the position on the chart of each frequency marker, the frequency, the ordinate (measured from one edge of the chart paper) of the derivative signal at even chart intervals, and the equation of the base line, which generally was not parallel to the edge of the paper.

Effect of Extra Line Width in the Superconductor

In deriving the signal response in the superconductor, we assumed that $g(\nu)$ remained constant. Actually, however, the resonance line was observed to widen when the sample became superconducting. Figure 6 shows the temperature dependence of the linewidth (measured between points of $\frac{1}{2}$ maximum absorption). Not only were the lines wider, but also, in the superconducting state, they showed broad wings. Since these wings saturated much more readily than did the center portions of the line, we believe that the signal in the wings arose from the portions of the sample near the surface of the spheres, where H_1 is strongest. The broadening characteristic of the surface could be two types, which require different treatments in determining an experimental relaxation time.

Homogeneous Broadening

In the normal state of gallium, the line broadening is produced by magnetic dipole-dipole interaction.[12] It is expected that, near the surface, the dipolar linewidth would be different from the value appropriate to the interior. At each point the line shape would be different. Each contribution would be centered at the same frequency in this approximation. In the saturation factor we may therefore use the observed value of $g(\nu)$; this approximation would be very good for an analysis of T_1. The foregoing analysis of the amplitude of the signal did not take into account the variation of $g(\nu)$; the apparent value of $\lambda(0)$ is therefore too small, but only by a few percent.

Inhomogeneous broadening,[32] resulting from a distribution of field gradients near the surface, appears to be a more likely possibility. This is clear, since a one percent change in field gradient would contribute an extra linewidth 1000 times greater than would a one percent variation in the dipole interaction. It is reasonable to assume that, although the interior regions of the spherical metal particles may be subject to some strains or imperfections, nevertheless the effects are predominant only near the surface. Let us consider that at each point in the sphere the line shape is identical to that in the normal metal. However, the center frequency of the symmetrical shape is a function of its position in the sphere. The observed signal will then be a summation of incremental signals, each from a small region. In general, the center frequency for each region will be different. The expression for the signal is then

$$S=\frac{n_0}{\int H_1^2 d\tau}\int_{\text{sample}}\int_{-\infty}^{\infty}\frac{F(\nu_i,\tau)g_N(\nu_i)H_1^2(\tau)d\tau_1 d\nu_i}{1+2\gamma^2H_1^2(\tau)T_1 g_N(\nu_i)},$$

where the line shape in the normal metal is $g_N(\nu_i)$, which is assumed to be characteristic of points far removed from the surface, and to result from magnetic dipole interactions. $F(\nu_i\tau)$ is the distribution function of the center frequency, i.e., the probability that the center frequency at a specified position in the sample is ν_i. (The frequencies are measured from the center of the observed line, neglecting any frequency shift arising directly from a superconducting property.) Since the observed lines were always symmetrical, we may assume that $F(\nu_i,\tau)$ is symmetric in ν_i about $\nu=0$. But we must consider an ensemble of frequencies at any one point, because the field gradient at some location near the surface will depend on the possible disorientation of the crystal axes there. Thus, while a given volume element is identical from sphere to sphere as far as the superconductivity is concerned, each sphere can have a different crystal orientation with respect to H_1, and thus a different field gradient at the same corresponding point in each sphere. This is true whether or not each sphere is a single crystal. In particular, we can assume $F(\nu_i,\tau)$ to be a Gaussian curve in frequency, where the width in frequency is a function of the particular $d\tau$. In the interior of a sphere, F is assumed to be narrow compared with the magnetic dipole width. Near the surface, however, the width of F becomes comparable to or somewhat greater than the dipole width. The magnetic dipole width will also change near the surface, but only by a negligible amount.

At rf powers below saturation, the effect of inhomogeneous broadening is qualitatively similar to that of homogeneous broadening, viz., we construct a function $\alpha(\tau)\equiv\int_{-\infty}^{\infty}F(\nu_i\tau)g_N(\nu_i)d\nu_i$, which behaves much like

[32] A. M. Portis, Phys. Rev. **91**, 1071 (1953).

the function $g(\nu,\tau)$ for the homogeneous case. Now both $\alpha(\tau)$ and $g(\nu,\tau)$ become equal to $g_N(\nu)$, the normal metal value, at interior points, and they both widen rapidly as the surface is approached. Therefore the conclusions regarding the value of $\lambda(0)$ are the same for both broadening mechanisms.

However, in analyzing the saturation data in order to obtain T_1, we must use $g_N(\nu)$, the normal, unsaturated line shape. The function $F(\nu_1,\tau)$ will change the shape of the saturation curve only slightly.

IV. THEORY OF RELAXATION

Relaxation Mechanisms

We proceed to enumerate the possible relaxation mechanisms, emphasing those which are pertinent to the study of quadrupole resonance in metals. In particular we consider the effect on the relaxation rate of the transition to the superconducting state.

We first eliminate from consideration the processes which predominate in insulators. These processes are related to lattice vibrations, and result, even at room temperature, in relaxation rates which are much slower than is characteristic of metals. Moreover, the rates observed in nonmetals[33] depend strongly on temperature (T^2 to T^7), in marked contrast to the behavior of metals,[34,35] in which relaxation rates are directly proportional to the first power of T. The relaxation processes which originate in lattice vibrations may therefore be neglected at low temperatures.

Mitchell[10] has considered the three principal interactions, which are of present concern, between the nuclei and conduction electrons: (1) the contact[36] part of the magnetic hyperfine interaction, (2) the noncontact part of the magnetic hyperfine interaction, and (3) the nuclear quadrupole coupling. In the first of these (which is usually dominant) both the nucleus and electron flip spins, conserving the total z component of spin; the noncontact term relaxes the nuclear spin, but total z component of spin is not conserved; and the quadrupole interaction changes the z component of the nuclear spin by either one or two units, leaving the electron spin unchanged. In all three cases, energy is conserved, since the conduction electron is scattered into a new state in k space near the Fermi surface. It is on this account that the relaxation experiments in the superconductors are interesting.

Mitchell calculates matrix elements in the Bloch approximation for each of the above terms, and determines the spin relaxation rate in the first order of perturbation. The total relaxation rate can be expressed as a sum of M, the magnetic hyperfine contribution (contact and noncontact), and Q, the quadrupole contribution. M is the coefficient of $w_m^{\pm}$ and Q is the coefficient of $W_m^{\pm 1}$ and $W_m^{\pm 2}$ in Mitchell's Eq. (13). (The numerical factor in M should be 1040/81.)

We first apply the calculation to the case of gallium, for which $I=\frac{3}{2}$, and find that the corresponding relaxation rate between quadrupole energy levels is $1/T_1=6(M+8Q)$; for comparison, Mitchell found, for $I=1$, $1/T_1=2(M+5Q)$. Both Q and M are proportional to the absolute temperature T.[36]

Relaxation Rate in a Superconductor

Magnetic Interaction

Hebel and Slichter[6] have treated the case in which the contact term is dominant. We now show that the effect of the noncontact term is similar. Consider the ratio of the relaxation rates in the superconducting and normal states[6];

$$\Re_S/\Re_N=\frac{2}{k_BT}\int_{\epsilon_0}^{\infty} f(1-f)dE(E^2\mp\epsilon_0^2)/(E^2-\epsilon_0^2).$$

Here, $E=(\epsilon^2+\epsilon_0^2)^{\frac{1}{2}}$, where the energy ϵ is measured relative to the Fermi energy, ϵ_0 is one-half the energy gap, and f is the Fermi function with argument E. The choice of sign in the numerator of the rate equation depends on the behavior of the single-electron scattering matrix element $B_{k,\sigma;k',\sigma'}$ in the BCS[9] framework. The lower (+) sign is obtained for the magnetic hyperfine terms, because the matrix elements of the operator either (1) produce an electron spin flip, $\sigma\neq\sigma'$, or (2) are spin-dependent such that $B_{k,\uparrow;k',\uparrow}=-B_{-k',\downarrow;-k,\downarrow}$, or (3) satisfy the condition $B_{kk'}=-B_{-k',-k}$. Referring to the three matrix elements in Mitchell's Eq. (10), the first two (which include the contact term) fall under (1) above, while part of the third satisfies (2) and the other part, (3). Therefore the temperature dependences of the noncontact and contact relaxation rates are identical, and

$$M_S/M_N=(2/k_BT)\int_{\epsilon_0}^{\infty} f(1-f)dE(E^2+\epsilon_0^2)/(E^2-\epsilon_0^2).$$

Hebel and Slichter used this expression in their discussion of the contact interaction. In order to avoid the divergence at $E=\epsilon_0$, they smeared out the electronic energy levels to a breadth Δ. Hebel[37] has calculated the ratio M_S/M_N in terms of T/T_c and a parameter $r=\epsilon_0(0)/\Delta$, where $\epsilon_0(0)$ is one-half of the energy gap at $T=0$. His curves show the general features of an initial enhancement just below T_c, followed by an exponential decrease. Redfield[7] has suggested that Δ may be interpreted as an anisotropy of ϵ_0 in k space.

Quadrupole Interaction

The matrix elements of the quadrupole interaction [Mitchell's Eqs. (7) and (8)] are independent of

[33] W. Blumberg, Phys. Rev. **119**, 79 (1960). N. Bloembergen, Physica **15**, 386(1949); G. Wikner, thesis, University of California, 1959 (unpublished).
[34] A. G. Redfield, Phys. Rev. **101**, 67 (1956).
[35] J. J. Spokas and C. P. Slichter, Phys. Rev. **113**, 1462 (1959).
[36] J. Korringa, Physica **16**, 601 (1950).
[37] L. C. Hebel, Phys. Rev. **116**, 79 (1959).

electron spin, and the scattering operators obey the relation $B_{k,k'}=+B_{-k',-k}$. This is the BCS "Case I," and the upper (−) sign in the rate equation gives

$$Q_S/Q_N=(2/k_BT)\int_{\epsilon_0}^{\infty} f(1-f)dE.$$

However, since $f(1-f)=-k_BTdf/dE$,

$$Q_S/Q_N=2f(\epsilon_0)=2[1+\exp(\epsilon_0/k_BT)]^{-1},$$

and we see that the quadrupole rate *drops* with infinite slope below T_c, in contrast with the *rise* which typifies the magnetic hyperfine rate.

The above expression for Q_S/Q_N is identical to the ratio α_S/α_N [BCS Eq. (4.29)] for the ultrasonic attenuation. It has been emphasized[6] that the contrasting behaviors of BCS Case II (magnetic relaxation) and Case I (ultrasonic attenuation) provide direct verification of the basic feature of the spin-momentum correlation of the BCS theory. In this connection it is interesting to point out the possibility of investigating both Cases I (Q) and II (M) in the same metal by the resonance method. We look for a metal possessing two isotopes, one of which has a large nuclear quadrupole moment, which will dominate its relaxation. In the following we show that Hg^{199} ($I=\frac{1}{2}$) and Hg^{201} ($I=\frac{3}{2}$) are a good pair of isotopes for such a study.

Relative magnitudes of M and Q may be estimated for several superconductors. In particular, we are presently interested in aluminum (Al^{27}), gallium ($Ga^{69,71}$), indium ($In^{113,115}$), and mercury ($Hg^{199,201}$). Following Mitchell, it is illuminating to compare first the noncontact with the contact part of the magnetic hyperfine interaction; this may be followed by a comparison of the quadrupole and noncontact terms.

Mitchell estimates the ratio of noncontact to contact relaxation rate to be $\alpha^4(10^{-21}/l^2)/(10^{-51}/l^6)$, where α is the ratio of the p- to s-wave contribution in the total wave function and l is a characteristic length of the order of 10^{-8} cm. The above ratio is equal to unity when $\alpha\approx 3$. Mitchell concludes that in multivalent metals the noncontact interaction may have an appreciable effect.

The ratio of the quadrupole to the noncontact term may be written

$$0.4C(Q/g)^2/[I(2I-1)]^2.$$

C is equal to 8 for the quadrupole level case of $I=\frac{3}{2}$; approximately 10 for $I=\frac{5}{2}$; and approximately 80 for $I=9/2$. Q is the nuclear quadrupole moment written in units of 10^{-24} cm^2; the nuclear g factor is written in units of the nuclear magneton. On this basis, the quadrupole term appears to be relatively small in Al, Ga, and In; it is appreciable in Hg^{201}, however.

Preliminary saturation measurements on the NQR of indium reveal no great decrease in the relaxation rate below T_c. The NQR of Hg^{201} has not yet been observed, and attempts are being made to find it, in the expectation that the quadrupole relaxation term will be strong enough to produce the expected sharp reduction in relaxation rate just below T_c. The other isotope, Hg^{199} ($I=\frac{1}{2}$), has no quadrupole moment, and would therefore be expected to behave as do Ga and Al.

V. EXPERIMENTAL RESULTS

Relaxation Rate

Normal State

Measurements were made at five temperatures between 4.2°K and 1.18°K, which is just above the critical temperature (1.084°) for gallium. The relaxation rate was observed to be proportional to temperature: The five experimental points scattered about a line through the origin (rate=0, $T=0$) with a maximum deviation of 7%, which is within experimental error.

Superconducting State

Measurements were made at eleven temperatures below T_c, the lowest temperature being 0.793°K, for which the reduced temperature $t=0.732$. The data are shown in Fig. 7, in which the rate is expressed relative to the rate which would be appropriate to the normal metal at the same temperature. The solid curve is from a theoretical calculation of Hebel.[37] We also include a single point, representing the maximum enhancement obtained in aluminum by Masuda and Redfield.[8]

Although the points in Fig. 7 are obtained from the data on the extreme assumption that the broadening is inhomogeneous, a further analysis, based on the behavior of the amplitude of the observed derivative signal, gives the same result within the estimated

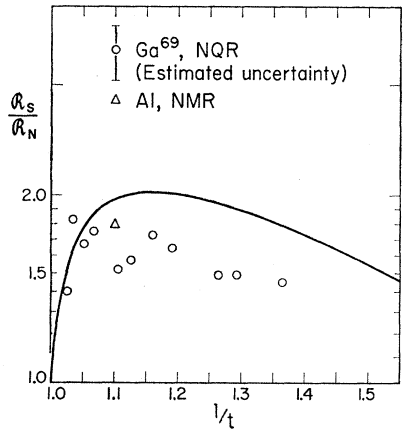

FIG. 7. The ratio of the relaxation times, superconducting to normal state, plotted vs the reciprocal of the reduced temperature. The solid curve is a theoretical calculation, based on BCS for $\epsilon_0(0)/\Delta=15$, by Hebel (reference 37). The value for aluminum was obtained from reference 8. The estimated uncertainty for all of the Ga^{69} data is indicated.

uncertainty. This is reasonable, since the variation in linewidth never exceeded ten or fifteen percent.

The experimental value of T_1 in the normal state between 1.1 and 4.2°K yields a value for T_1T of 0.4 sec-°K, which is in agreement with independent pulse[38] measurements. This is expected to be somewhat larger than the value ($T_1T \approx 0.2$) which is estimated by means of Korringa's formula, since the latter must rely on measurements in the liquid metal, which possesses a different electronic structure.[39] Although the errors in the separate determinations of $\mathcal{R}_S$ and $\mathcal{R}_N$ may be appreciable, they are largely eliminated in the ratio $\mathcal{R}_S/\mathcal{R}_N$, which we believe to be as reliable as is indicated in Fig. 7.

Conclusions Concerning $\mathcal{R}_S/\mathcal{R}_N$

We find that the quantity $\mathcal{R}_S/\mathcal{R}_N$ for gallium reaches a peak value of 1.8 at $T/T_c \approx 0.95$. This is consistent with the results obtained by others for aluminum, and we may interpret the effect in terms of an energy gap in the excitation spectrum of the superconductor. The observed *peak* justifies our expectation that the quadrupole interaction does not dominate the relaxation process.

The curve of $\mathcal{R}_S/\mathcal{R}_N$ vs temperature corresponds to a value of 10 for the energy level breadth parameter $r = \epsilon_0/\Delta$. Here Δ may be associated with electron scattering processes,[6] in which case the peak value of $\mathcal{R}_S/\mathcal{R}_N$ should depend on the purity and size of the sample particles. Alternatively one may relate Δ and the anisotropy of the energy gap, but the present data are not sufficient to distinguish between these interpretations. We might argue, for example, that an isotropic energy gap requires that the electronic specific heat be a simple exponential function of temperature, and conversely that deviations from a simple exponential form constitute evidence for an anisotropic gap. On this basis, gallium, whose crystalline properties are notably anisotropic, should be expected to exhibit deviations from the simple exponential specific heat; and aluminum, which is cubic, should behave more like an isotropic material. The experimental facts[40,41] for these two metals, however, are just the reverse of what the foregoing argument leads us to expect, and we must conclude that further evidence is required before the role of Δ is to be understood fully.

Frequency Shift of the NQR in Superconductors

The frequency of the NQR changes in the superconducting transition. Figure 8 shows the relative values of the shift as a function of temperature. The absolute change in frequency is only 620 cps, which is approximately one tenth of the linewidth. In spite of its smallness, we believe that the change in frequency is a real effect in the superconductor which does not arise from a change in line shape. It is true that, if the field gradients near the surface of the metal spheres were for example higher than in the interior portions, a positive shift would result. However, this would also require a change in the line symmetry. It is easy to show that the observed asymmetry of the line is too small to account for the frequency shift, viz.: An apparent frequency change of this kind will be approximately $\Delta f = \frac{1}{2}w(p^+ - p^-)/(p^+ + p^-)$, where w is the linewidth between derivative peaks, whose amplitudes are p^+ and p^-. In this experiment, the Δf resulting from the observed p^+ and p^- turns out to be less than one tenth of the observed frequency shift. Furthermore, the temperature dependence of the shift is different from that of the linewidth; the two effects are believed not to be related.

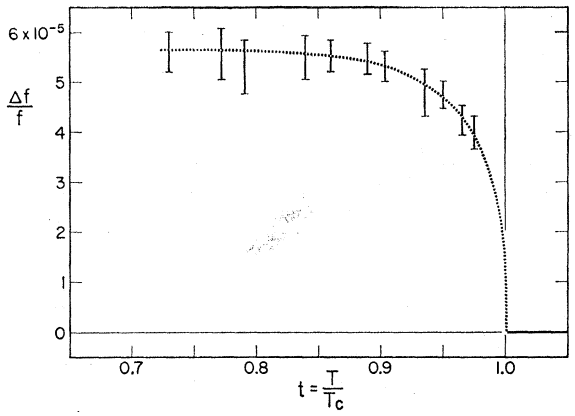

FIG. 8. The observed relative change of the NQR frequency of Ga^{69}, plotted vs the reduced temperature.

One might seek an explanation of the NQR frequency shift in terms of the volume change at the superconducting transition. But although the volume change has not been measured for gallium, it may be expected to be similar to other metals that have been investigated,[42,43] for which the change is too small and furthermore in the wrong direction to account for the present result. The evidence for this point is clearer for the case of indium,[44,45] for which we obtain a frequency shift of approximately -0.6% at a reduced temperature of 0.8. This is one hundred times larger than the corresponding effect in gallium. It is furthermore in the opposite direction. The known volume change of indium in the transition is four orders of magnitude too small to account for the frequency shift. The frequency shift in indium is larger than the linewidth and is therefore not subject to corrections for distortion in the line shape.

[38] L. Sarles (private communication) (see also reference 39).
[39] W. D. Knight, A. G. Berger, and V. Heine, Ann. Phys. 8, 173 (1959).
[40] N. Phillips, Phys. Rev. 114, 676 (1959).
[41] We are indebted to Dr. Phillips for communicating his preliminary results on gallium.
[42] J. L. Olsen and H. Rohrer, Helv. Phys. Acta 30, 49 (1957).
[43] G. D. Cody, Phys. Rev. 111, 1078 (1958).
[44] Preliminary results were obtained by Dr. R. Hewitt.
[45] C. P. Slichter and W. W. Simmons (private communication).

The evidence is quite convincing that the NQR frequency shift is a direct consequence of a modification of the electric field gradient produced by the conduction electrons in the superconductor. The conduction electrons, because of the energy gap, are distributed differently in k space in the superconductor, and this can produce a change in the quadrupole interaction. The fact that the frequency shifts in gallium and indium are of opposite sign can be reconciled if one realizes that the total field gradient in a metal may arise alternatively from situations in which the conduction electrons may either add or subtract from the crystalline contributions. Further experimental and theoretical work is in progress.

ACKNOWLEDGMENTS

We wish to acknowledge the contributions of Dr. R. R. Hewitt and Dr. L. R. Sarles during the preliminary stages of the work. Dr. M. Pomerantz suggested the use of the chopper calibrator and provided many stimulating conversations. Mr. A. B. Cecil kindly assisted with the necessary computing. The advice of Dr. John Thomas, of the California Research Corporation, was helpful to us in preparing and stabilizing the samples.

APPENDIX A: UNSATURATED SIGNAL IN A SUPERCONDUCTOR

The ratio of the signal (no saturation) in the superconductor to the signal in the normal state is

$$R=[\tfrac{4}{3}\pi r_0^3(H_1^N)^2]^{-1}2\pi\int_0^{r_0}\int_0^{\pi}H_1^2r^2dr\,\sin\theta d\theta,$$

H_1^N is the applied rf magnetic field. For a sphere of radius r_0 the solution to London's equation gives[46]

$$H_1^2/(H_1^N)^2=A\cos^2\theta+B\sin^2\theta,$$

where

$$A=(9\chi_0^2/\sinh^2\chi_0)(\sinh^2\chi/\chi^4)(1/\chi-\coth\chi)^2,$$
$$B=(9\chi_0^2/\sinh^2\chi_0)(\sinh^2\chi/\chi^4)\tfrac{1}{4}(1/\chi-\coth\chi+\chi)^2,$$
$$\chi=r/\lambda,\quad\text{and}\quad\chi_0=r_0/\lambda.$$

Integration over the angular dependence results in:

$$R=\chi_0^{-3}\int_0^{\chi_0}(A+2B)\chi^2d\chi.$$

One may then express A and B in terms of the series expansion of $\sinh 2\chi$ and $\cosh 2\chi$. The term-by-term integration is then trivial. After considerable rearranging, the desired expression is

$$R=\frac{9\chi_0^2}{\sinh^2\chi_0}\sum_{n=0}^{\infty}\frac{(2\chi_0)^{2n}(n^2+3n+4)}{(2n+3)!(n+2)(n+3)},$$

This is simply the average square field for unit external field in a superconductor, assuming that London's equations are valid; i.e., $R=\langle H^2\rangle_{\rm av}/H_0^2$, where H_0 is the external applied field.

$R(\chi_0)$ is plotted in Fig. 2.

APPENDIX B: SATURATED SIGNAL IN A SUPERCONDUCTOR

We wish to calculate the ratio of the signal in the superconductor with saturation to the signal in the normal state with no saturation:

$$R_1=[\tfrac{4}{3}\pi r_0^3(H_1^N)^2]^{-1}\int(1+cH_1^2)^{-1}H_1^2d\tau_1,$$

where $c=2\gamma^2T_1g(\nu)$, and

$$H_1^2/(H^N)^2=A\cos^2\theta+B\sin^2\theta,$$

as in Appendix A. Integration over θ gives

$$R_1=(\tfrac{2}{3}b\chi_0^3)^{-1}\int_0^{\chi_0}f(\chi)d\chi,$$

where

$$b=2\gamma^2T_1g(\nu)(H_1^N)^2,$$
$$\chi=r/\lambda,\quad\chi_0=r_0/\lambda,$$

and

$$f(\chi)=2\chi^2-\frac{\chi^2}{[b(B-A)(1+bB)]^{\frac{1}{2}}}\times\ln\frac{(1+bB+[b(B-A)(1+bB)]^{\frac{1}{2}})}{(1+bB-[b(B-A)(1+bB)]^{\frac{1}{2}})}.$$

This was integrated numerically on a computer for 9 values of χ_0 and 10 values of b. These results were divided by R (see Appendix A), which is equal to R_1 for $b=0$, to give the saturation parameter, Z_s, for the case of a superconductor. A plot of Z_s for one value of χ_0 is shown in Fig. 4.

[46] D. Shoenberg, *Superconductivity* (Cambridge Uuiversity Press, New York 1952), p. 234.